

DISCLAIMER

This report was prepared as an account of work sponsored by an agency of the United States Government. Neither the United States Government nor any agency thereof, nor any of their employees, makes any warranty, express or implied, or assumes any legal liability or responsibility for the accuracy, completeness, or usefulness of any information, apparatus, product, or process disclosed, or represents that its use would not infringe privately owned rights. Reference herein to any specific commercial product, process, or service by trade name, trademark, manufacturer, or otherwise does not necessarily constitute or imply its endorsement, recommendation, or favoring by the United States Government or any agency thereof. The views and opinions of authors expressed herein do not necessarily state or reflect those of the United States Government or any agency thereof.

CONF-861061--1

NEUTRON DECAY OF GIANT RESONANCES IN ^{208}Pb .

DE87 006620

A. Bracco

Dipartimento di Fisica, Universita di Milano, 20133 Milano, Italy

and

J.R. Beene, P.E. Bertrand, M.L. Halbert, R.L. Auble, D.C. Hensley,
D.J. Horen, R.L. Robinson, and R.O. Sayer

Oak Ridge National Laboratory, Oak Ridge, Tennessee 37830, USA.

ABSTRACT

The neutron decay of the giant multipole resonance region between 9 to 15 MeV in ^{208}Pb has been studied. The giant resonances were excited by inelastic scattering of ^{17}O at 380 MeV. Neutrons from ^{208}Pb and γ rays from $^{207}\text{Pb}^*$ were detected in the ORNL Spin Spectrometer and the ^{17}O in ΔE -E silicon detector telescopes. The neutron branching ratios for the decay to the ground state and to the low lying excited states of ^{207}Pb were measured as a function of the excitation energy of ^{208}Pb and compared to Hauser-Feshbach calculations. Evidence for non statistical neutron decay to selected single-hole states, and to hole-surface vibration and hole-pairing vibration coupled states was found.

1. INTRODUCTION

A giant vibration can be viewed as a correlated state of a particle above the Fermi surface and a hole in the Fermi sea. These states are located in general at excitation energies above the particle binding energies and therefore they decay predominantly by charged particle and neutron emission in light nuclei and, due to the Coulomb barrier, only by neutron emission in heavier nuclei. Gamma decay is also possible, but the relative decay branch goes from 10^{-3} to 10^{-5} . The coupling of the 1p-1h state to the continuum gives rise, for the excitation of closed shell nuclei, to the direct decay into the hole states of the (A-1) nucleus with partial width given by the escape width Γ' (cfr. figure 1). The 1p-1h states can couple through the

MASTER

INSTRUCTION OF THIS DOCUMENT IS UNLIMITED

residual interaction to more complicated states present in the vicinity of the resonance. Two particle-two hole states, referred to as doorway states, represent the first step of the damping process of the resonance toward the compound nucleus. For closed shell nuclei, the 2p-2h states containing a pair of uncorrelated fermions and low lying surface vibrations or collective pairing modes are expected to be important doorway states (refs. 1,2). The 2p-2h states couple again to more complicated states until a completely equilibrated system is reached. Particle decay can thus occur either directly from the giant resonance or at any of the intermediate levels of the damping process or from fully equilibrated compound states. As a consequence, the comparison of the experimental neutron decay branching ratio with the statistical model predictions for states of the A-1 nucleus having different nuclear structure can be used to study both the microscopic structure and the damping process of giant resonances.

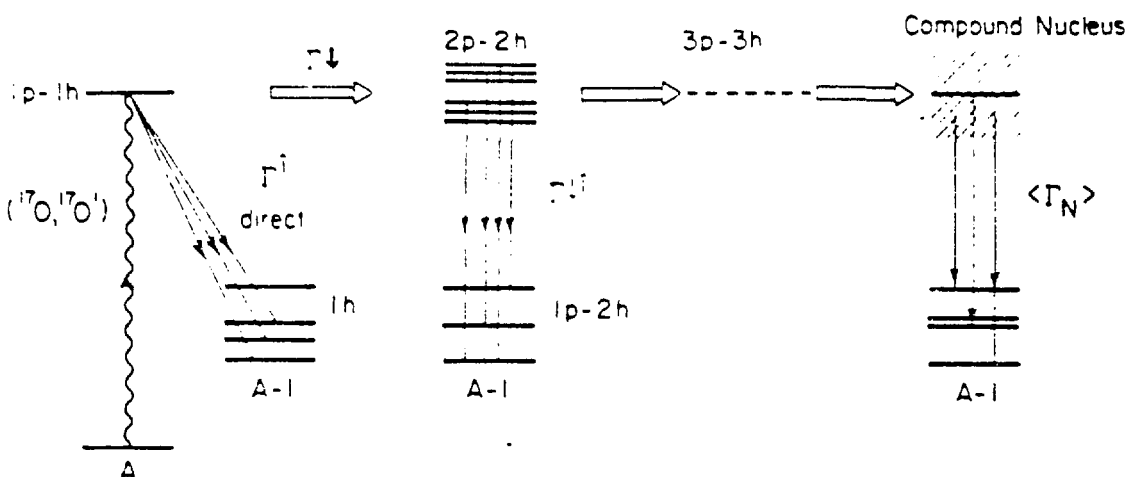


Fig. 1. Illustration of neutron decay from a giant resonance state. Γ^1 is the direct escape width, Γ^2 is the spreading width, Γ^3 is the escape width from intermediate states of the damping process of the giant resonance. $\langle \Gamma_N \rangle$ is the decay width from the compound nucleus.

The experiment reported here is concerned with the measurements of the neutron decay of the giant multiple resonance region (9-15 MeV of excitation energy of) ^{208}Pb . The neutron branching ratios for the decay to the low-lying hole states and particle vibration coupling states (1p-2h) were measured as a function of ^{208}Pb excitation energy and were compared to the Hauser-Feshbach predictions.

In previous studies of neutron decay from the giant resonance region of ^{208}Pb (refs. 3,4,5,6) the comparison of the neutron energy spectra with statistical model calculations indicates the presence of a small non statistical neutron branch in the giant monopole resonance region. However, a more recent statistical model analysis (ref. 7) of the data of reference 6 suggests the absence of non-statistical decay. The lack of good statistics and energy resolution of these measurements did not allow the study of the neutron branching decay ratios to individual states in ^{207}Pb as

a function of ^{206}Pb excitation energy.

The present experiment differs in two important aspects from the previous ones; first, by using inelastic scattering of heavy ions the GQR and GMR are strongly excited, and second the decay studies were made for a number of well resolved 1h and 1p-2h final states.

2. THE EXPERIMENT

In the present study, the resonances were excited by inelastic scattering of 380 MeV ^{17}O . This reaction resulted in a large excitation cross section for the the quadrupole and monopole resonances in comparison with the underlying continuum.

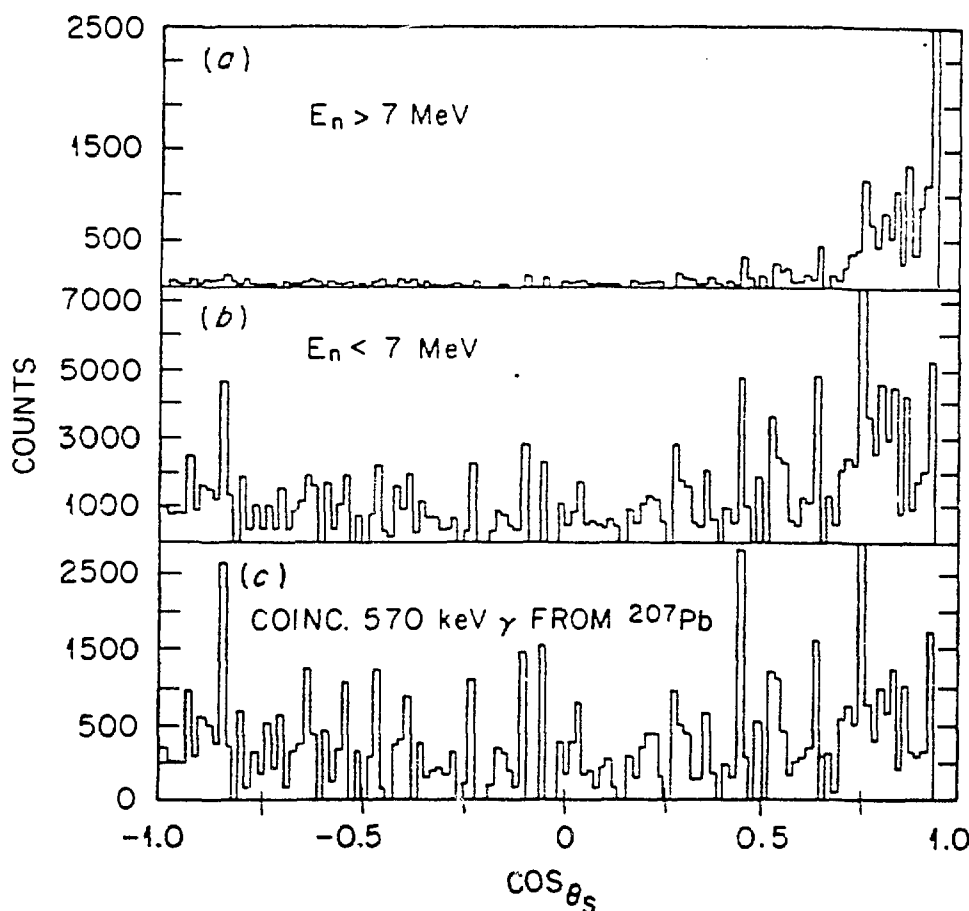


Fig.2. Neutron angular distributions for different neutron kinetic energies E_n (parts (a) and b)). θ_S is the neutron angle with respect to the scattered ^{17}O . The angular distribution shown in part c is that of neutrons decaying from ^{208}Pb at excitation energy 9-15 MeV and populating the first excited state (570 KeV) in ^{207}Pb .

The inelastically scattered ^{17}O was detected in six cooled Si surface-barrier telescopes arranged symmetrically around the beam at an angle of 13° and subtending $\Delta\theta = 3^\circ$ and $\Delta\phi = 9^\circ$ each and a total solid angle of 22.6 msr . The telescopes consisted of two elements of thickness 0.5 mm and 1. mm, respectively. The energy resolution was 800 KeV and the mass resolution sufficient to separate ^{17}O from adjacent oxygen isotopes. Neutrons and gamma rays were detected in 70 elements of the ORNL Spin Spectrometer (ref. 8). The spectrometer consists of a spherical shell of NaI 17.8 cm thick, divided into 72 independent modules surrounding the target chamber.

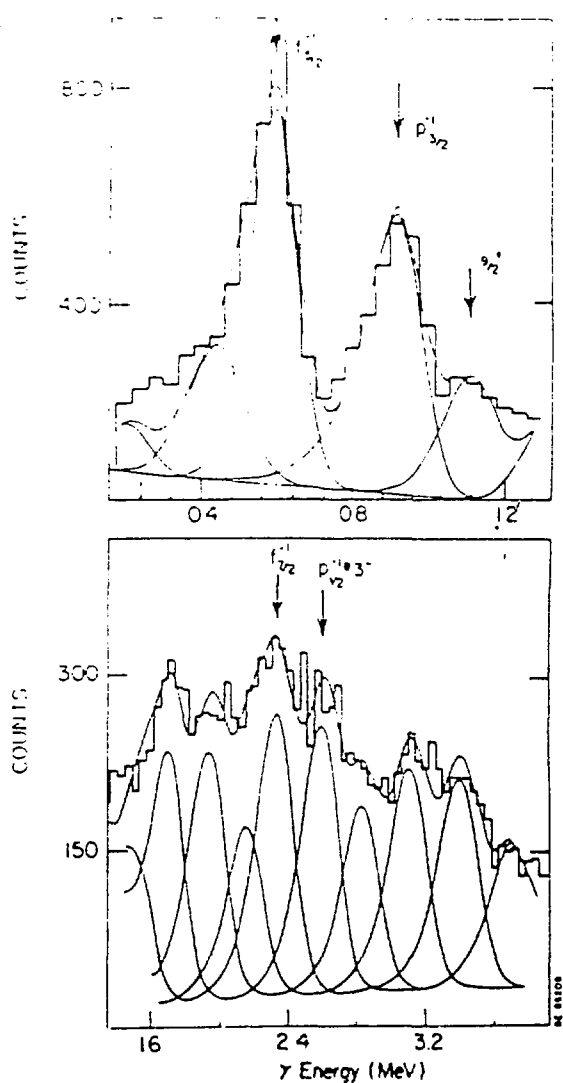


Fig. 3. Sum Gamma energy spectrum for ^{208}Pb excitation energy of 12-13 MeV. The states indicated by the arrows are the ones having known decay branchings to the ground and isomeric states.

The raw data obtained from the spectrometer consisted of pulse heights from the individual NaI elements and times of these pulses relative to the inelastically scattered ^{17}O with which they were in coincidence. The total gamma ray pulse height was obtained by summing all those pulses which occurred in a prompt time window. This window (which was a function of pulse height) was narrow enough to eliminate pulses resulting from detection of neutrons with energy less than $\sim 7 \text{ MeV}$. Because of the short flight path, the energy resolution from neutron time of flight is insufficient to distinguish individual levels in ^{207}Pb . The residual excitation energy in ^{207}Pb after neutron emission is, however, accurately determined from the sum gamma ray energy in the spin spectrometer. The events of interest for the present study were thus identified by the presence of neutrons (i.e. delay pulses in the NaI), and by a total γ energy deposited in the Spin Spectrometer equal to one of the ^{207}Pb level energies and ^{17}O with kinetic energy corresponding to excitation energy of ^{208}Pb above one neutron emission threshold (7.4 MeV). Although redundant, the detection of neutrons is used for discriminating against contributions from processes

other than inelastic excitation followed by neutron decay. The investigation of these processes was made by considering angular distributions. Figure 2a shows the angular distribution with respect to the direction of the scattered particle of the pulses from the spin spectrometer with an apparent gamma energy larger than 7 MeV (at these energies is not possible to distinguish between neutrons and gammas by time of flight). The fact that these events are tightly distributed around the direction of the scattered particles suggests that these are neutrons from the ($^{17}\text{O}, ^{18}\text{O}'$) neutron pick up process in which the ^{18}O decays by neutron emission while in flight toward the detector (sequential decay). Such a process should produce neutrons moving approximately at the beam velocity ($E_n \sim 21$ MeV) which would not be identified by time of flight and which would often deposit large energies in the NaI detectors. The angular distribution of neutrons (i.e. delayed pulses) for ^{208}Pb excitation energy larger than 8 MeV and with energy less than ~ 7 MeV is shown in figure 2b. A forward-backward asymmetry is seen in the data. In the case of the angular distribution of neutrons corresponding to population of the first excited state in ^{207}Pb , and for ^{208}Pb excitation energy from 9 to 15 MeV, the forward-backward asymmetry is

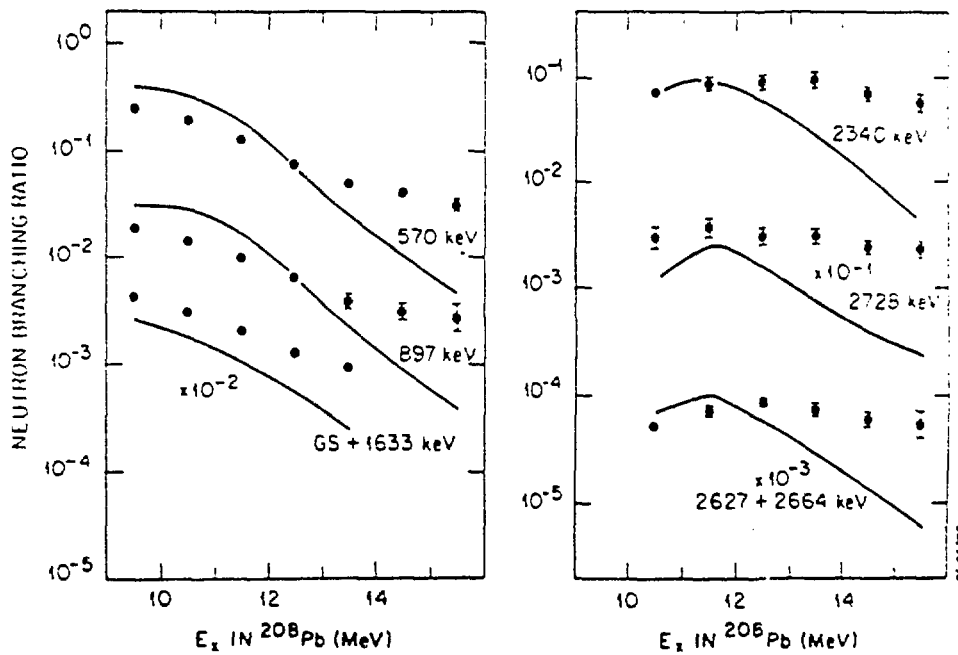


Fig.4. Neutron branching ratios obtained with the present measurements as a function of ^{208}Pb excitation energy for given excited states in ^{207}Pb . The curves are the Hauser Feshbach predictions described in the text.

much less enhanced (cf. fig. 2c). This asymmetry is typical of non statistical decay. However, it is important, as a first step of the study, to restrict the analysis to a region free of any contaminations from scattered high energy neutrons from the neutron pick up and sequential decay mechanism, which might be present in the forward hemisphere. Another potential mechanism for production of neutrons unrelated to giant resonance decay is the knockout reaction. Such a process is expected

to produce neutrons peaked near the target recoil direction (ref. 9). No evidence for a significant yield of such neutrons (at $\sim 85^\circ$ deg in this case) was found.

The present analysis is therefore based on a determination of the initial ^{208}Pb excitation energy from the scattered ^{17}O energy, the detection of a neutron in the Spin Spectrometer (identified by time of flight) in the backward hemisphere, and the determination of the residual ^{207}Pb excitation energy by total gamma energy emitted as prompt radiation, detected by the Spin Spectrometer. A sample of total gamma energy spectrum is shown in figure 3, corresponding to an excitation energy of 12-13 MeV in ^{208}Pb . The spectrum was fitted with gaussians whose centroids are either at the energy of known excited states in ^{207}Pb or at the energy difference of known states from 1.633 MeV, the energy corresponding to the isomer state $11/2^-$ of ^{207}Pb . Since the isomer could not be distinguished from the ground state, the deexcitation the ^{207}Pb levels which could go through the isomeric state were included in the analysis in this way. The peaks indicated by the arrows in figure 3 are the ones that are better separated from the others and correspond to states in ^{207}Pb for which the branching decay ratio to the ground state and to the isomeric state is well known. In addition, the nuclear structure of these states is known. The neutron branching ratios at a given ^{208}Pb excitation energy for the decay to a particular ^{207}Pb state was obtained from the area of the corresponding gaussian in the sum energy spectrum divided by the number of ^{17}O single events at the same ^{208}Pb excitation energy. Corrections for neutron and gamma efficiency were applied.

The efficiency of the Spin Spectrometer for neutron detection (45% on average up to 7 MeV neutrons) was measured by the ratio of the gamma yields from the first excited state of ^{207}Pb with and without the presence of neutrons (delay pulses) at different ^{208}Pb excitation energy bites. The gamma total and photopeak efficiencies were measured detecting gamma events from ^{207}Bi , ^{88}Y , and ^{60}Co sources in the same experimental configurations. The obtained values are in agreement with the ones reported in reference 8.

3. RESULTS AND DISCUSSION

The measured neutron branching ratios for the decay to the ground plus the isomeric states, to the 570 KeV ($5/2^-$), the 890 KeV ($3/2^-$), and the 2340 KeV ($7/2^-$) states, to the surface vibration coupling 2623 and 2665 KeV doublet, and to the pairing vibration coupling 2728 KeV state are shown in figure 4. The error bars contain the statistical and peak fitting uncertainties. For the 570 and 890 KeV states, the yield of events corresponding to the deexcitation of higher excited states through the emission of two or more gamma rays and with the detection of only the 570 or 890 KeV gamma rays were subtracted. These corrections amount to only a few percent.

The Hauser-Feshbach predictions are also presented in figure 4. The calculations were made using the optical model potential of reference 10, the

experimentally known levels of ^{207}Pb up to 4 MeV and, above this energy, the level density of reference 11 which gives a good account of the experimental data in the relevant

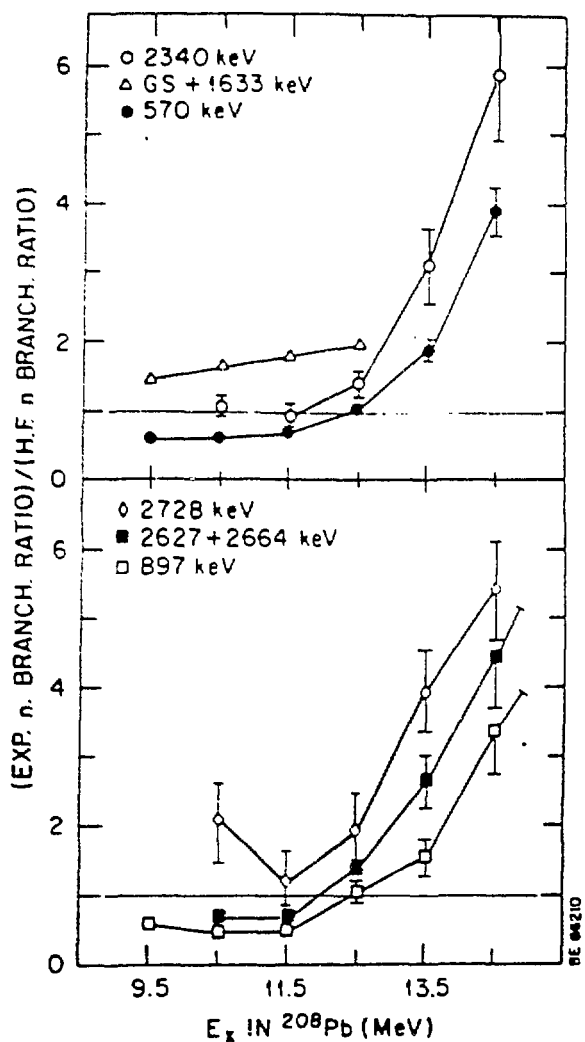


Fig.5.Ratio of the experimental and calculated neutron branching ratios as a function of ^{208}Pb excitation energy for given low lying excited states in ^{207}Pb . Straight lines are drawn between the points to guide the eyes.

spin and excitation energy range. The calculations are linear combinations of neutron branching ratios for ^{206}Pb states of multipolarity 0,1,2,3,4. The strength distribution for multipolarities up to 4 was taken from (p,p') data (ref. 12). Making use of the fraction of the EWSR reported in reference 12, the cross sections for ($^{17}\text{O},^{17}\text{O}'$) at 13^0 were calculated using DWBA. Except for an almost constant underlying continuum, this distribution of $L=0-4$ strengths provides a good account of the experimental inelastic spectrum for ^{208}Pb excitation energies in the 9 to 15 MeV region of interest here. The effects of the decay of this continuum is not included in the calculation. The strength distribution used and the calculated DWBA cross sections are given in table I.

The general trend of the present measurements is shown in figure 5, where the ratios of the experimental and calculated neutron decay branching ratio are plotted. The differences between experiment and statistical predictions in the ^{208}Pb excitation energy region < 12 MeV are smaller than the ones in the higher energy region. Near to the neutron emission threshold, the statistical calculations are very sensitive to the

values of the transmission coefficient which at these very low neutron energies have significant sizes only for small neutron orbital angular momenta. The calculations of the transmission coefficients obtained making use of the neutron strength functions of reference 13 differ from the ones obtained with the optical potential only by few percent and cannot improve the agreement between experiment and statistical calculations in the ^{208}Pb excitation energy region < 12 MeV. However, if addition of

$L=6$ strength is made, as previously suggested (refs. 2 and 14), the calculations describe better the data up to 12 MeV ^{208}Pb excitation energy with the exception of the first excited state (ref. 15). For ^{208}Pb excitation energies from 12 to 15 MeV there is a net excess of the experimental branching ratios over that calculated. At these excitation energies the statistical model calculations are very sensitive to the value used for the level density of ^{207}Pb , the neutron transmission coefficient being almost one. The experimental neutron branching ratios can be reproduced by the statistical model calculations only if a level density at least a factor of 5 smaller is used. Such a small value is inconsistent with the measured level density. In addition, the enhanced neutron branching ratio does not depend on the nature of the ^{207}Pb states.

The neutron decay to various low lying states in ^{208}Pb leads to different information concerning the giant resonances in ^{208}Pb . The neutron branching ratios to ^{207}Pb hole states (G.S., 570 KeV, 890 KeV, 1633 KeV, 2340 KeV) could be used to obtain information about specific particle-hole amplitudes of the wave function describing the giant resonances. On the other hand, the neutron branching ratios to the 2600 KeV and 2728 KeV ^{207}Pb particle vibration states can be used to extract information on the 2p-2h doorway states by which the giant resonances are expected to couple to the compound nucleus.

$^{208}\text{Pb } E^*$ (MeV)	Γ (MeV)	L	%EWSR	σ (mb)
8.11	0.4	4	3	3.85
8.35	0.4	4	4	3.79
8.86	0.4	2	7	5.73
9.34	0.4	2	5	3.42
10.6	2.	2	70	30.3
12.0	2.4	4	10	7.41
13.6	4.0	1	100	4.36
13.9	2.9	0	100	10.0

Table 1. Energies, widths, multipolarities, and fractions of the energy weighted sum rules of the giant resonances in ^{208}Pb . In the last column the cross sections for excitation of the giant resonances with ^{17}O are given.

The collective vibration for the two states are the low lying octupole vibration and the pair removal mode of ^{208}Pb , respectively (cf. refs. 16 and 17). It will therefore

be interesting to compare the non-statistical decay of the giant resonances in ^{208}Pb for particular ^{207}Pb final states to theoretical predictions, when they become available. The latter comparison will provide a powerful tool to study the microscopic structure of giant resonances (ref. 18) at different levels of complexity in its decay toward the compound nucleus.

REFERENCES

1. G.F. Bertsch, P.F. Bortignon and R.A. Broglia, Rev. Mod. Phys. 55, 287(1983)
2. P.F. Bortignon and R.A. Broglia, Nucl. Phys. A371,405(1981)
3. A. van Der Woude, Nuclear Structure 1985, R. Broglia, G.B. Hagemann and B. Herskind editors, p.489
4. W. Eyrich, A. Hofmann, U. Scheib, S. Schneider, F. Vogler, and H. Rebel, Phys. Rev. Lett. 43,1369(1979).
5. H. Steuer, W. Eyrich, A. Hofmann, H. Orner, U. Scheib, R. Stamminger, D. Steuer, and H. Rebel, Phys. Rev. Lett. 47,1702 (1981).
6. W. Eyrich, K. Fuchs, A. Hofmann, U. Scheib, H. Steuer, and H. Rebel, Phys. Rev. C 29,418(1984)
7. H. Dias and E. Wolynec, Phys. Rev. C30,1164(1984)
8. M. Jaaskelainen, D.G. Sarantites, R. Woodward, F.A. Dilmaman, J. T. Hood, R. Jaaskelainen, D.C. Hensley, M.L. Halbert, and J.H. Barker, Nucl. Instrum. Meth. 204,385(1983).
9. H. Ejiri, Journal de Physique 45,C4-135(1984).
10. C.M. Perey and F.G. Perey, Atomic Data and Nucl. data Tables 17,1(1985).
11. A. Gilbert and A. G. W. Cameron, Can. Jour. of Phys. 13,1116(1963).
12. F. E. Bertrand, E.E. Gross, D.J. Horen, R.O. Sayer, T.P. Sjorenn, D. K. McDaniels, J. Lisanti, J.R. Tinsley, L. W. Swenson, J.B. McClelland, T.A. Carey, K. Jones, and S.J. Seestrom-Morris, Phys. Rev. C34,45(1986).
13. D.J. Horen, J.A. Harvey, and N.W. Hill, Phys. Rev. C18,722(1978).
14. H.P. Morsch, P. Decowski, M. Rogge, P. Turek, L. Zemco, S.A. Martin, G.P.A. Berg, W. Hurlmann, J. Meissburger, and J.G. Romer, Phys. Rev. C28, 1947(1983).
15. J.R. Beene, A. Bracco, F.E. Bertrand, M.L. Halbert, D.C. Hensley, R.L. Auble, D.J. Horen, R.L. Robinson, T.P. Sjoreen, R.O. Sayer, Phys. Div. Prog. Rep. for Period Ending Sept. 30,1986, ORNL and to be published.
16. D.R. Bes and R.A. Broglia, Phys. Rev. C3,2389(1971).
17. I. Hamamoto, Phys. Rep.10,63(1974).
18. R.A. Broglia and P.F. Bortignon, Giant Multiple Resonances, Ed. F.E. Bertrand, Harwood Ac. Publisher, New York (1979)317.